International Journal of Heat and Mass Transfer 104 (2017) 328–336

Contents lists available at ScienceDirect

International Journal of Heat and Mass Transfer

journal homepage: www.elsevier.com/locate/ijhmt

Analysis of the anomalies in graphene thermal properties

Khalil Khanafer [a], Kambiz Vafai [b,*]

[a] Biomedical Engineering Department, University of Michigan, Ann Arbor, MI 48109, USA
[b] Mechanical Engineering Department, University of California, Riverside, CA 93210, USA

ARTICLE INFO

Article history:
Received 30 June 2016
Received in revised form 27 July 2016
Accepted 28 July 2016

Keywords:
Graphene
Thermal conductivity
Nanoscale

ABSTRACT

A comprehensive analysis of the thermal conductivity of graphene under various conditions is presented in this study. Results obtained from different experimental and theoretical methods are analyzed and discussed for numerous conditions such as preparation process, shape, sample size, wavelength, and temperature. Wide discrepancies in the measured thermal conductivity results were found in many studies in the literature. Based on the cited data for the graphene thermal conductivity, the initially measured thermal conductivities appear to be highly overestimated. Majority of the documented results reported lower values of thermal conductivity than the earlier reported results. Furthermore, large differences in the values of the thermal conductivity of graphene were noticed from the cited results using different experimental and numerical methods (0.14 W/m K–20,000 W/m K). This raised an important question on the accuracy of these methods when measuring thermal conductivity of graphene at nanoscale. We have established the existence of a high degree of anomalies in the value of the thermal conductivity of grapheme. Therefore, proper experimental and theoretical studies should be conducted to accurately measure the thermal conductivity of graphene.

1. Introduction

Graphene, a single layer of carbon atoms bonded in a hexagonal lattice, is considered an excellent conductor of heat and electricity. Among its significant properties, an extremely high thermal conductivity, it has received voluminous attention in scientific and industrial fields over the last decade both experimentally and theoretically [1–12]. This consideration stems from its importance in a variety of important applications such as thermal management and electronic interconnects application [1–4,13–30].

There have been several works discussing the topic of graphene in recent years. For example, Castro Neto et al. [3] considered the basic theoretical aspects of graphene with unusual two-dimensional Dirac-like electronic excitations. Ma et al. [31] focused on recent progress in the synthesis of graphene nanoribbons (GNRs) by different techniques, especially longitudinal unzipping of carbon nanotubes (CNTs). The mechanical, electronic, and magnetic properties and edge reconstruction of GNRs are briefly summarized as well. Choi et al. [32] presented a study on the advancement of research in graphene, in the area of synthesis, properties and applications such as field emission, sensors, electronics, and energy, the limitations of present knowledge base and future research directions. A study of fundamental electronic properties of two-dimensional graphene with an emphasis on density and temperature-dependent carrier transport in doped or gated graphene structures was provided by Das Sarma [33]. The main feature of that work was a critical comparison between carrier transport in graphene and two-dimensional semiconductor systems (e.g., hetero-structures, quantum wells, inversion layers) so that the unique features of graphene electronic properties arising from its gapless, mass-less, chiral Dirac spectrum were highlighted.

Zhang et al. [34] summarized the recent advances in the study of graphene edges, including edge formation energy, edge reconstruction, method of graphene edge synthesis and the recent progress on metal-passivated graphene edges and the role of edges in graphene CVD growth. The aim of their work was to provide a guideline for readers to gain a clear picture of graphene edges from several aspects, especially the catalyst-passivated graphene edges and their role in graphene CVD growth. Recently, Renteria et al. [35] considered the thermal properties of graphene, few-layer graphene and graphene nanoribbons, and discussed practical applications of graphene in thermal management and energy storage. It was shown that the use of liquid-phase-exfoliated graphene as filler material in phase change materials was promising for thermal management of high-power-density battery packs.

* Corresponding author.
E-mail address: vafai@engr.ucr.edu (K. Vafai).

http://dx.doi.org/10.1016/j.ijheatmasstransfer.2016.07.103
0017-9310/

However, the thermal conductivity measurements of graphene reported to date exhibited contradictory results. For example, Balandin et al. [12] and Ghosh et al. [36] reported that the thermal conductivity of graphene measured by Raman Spectroscopy were 4840–5300 W/m K (2–5 μm diameter) and ~3080–5150 W/m K (1–5 μm diameter), respectively. On the other hand, Lee et al. [37] reported that the thermal conductivity of a suspended pristine graphene measured by the same method was ranging from ~1800 W/m K near 325 K to ~710 W/m K at 500 K. Moreover, Faugeras et al. [11] reported that the thermal conductivity of a suspended graphene disk 44 μm in diameter measured by the same method was 632 W/m K. Although the diameter of the suspended disk used by Faugeras et al. [11] was about nine times the diameter of the graphene used by Balandin et al. [12], the conductivity obtained by Faugeras et al. was about eight times smaller than that obtained by Balandin et al. [12]. Other experimental methods such as microelectrothermal system and scanning thermal microscopy reported values of graphene thermal conductivity in the range of 10–2500 W/m K [38–40,5,41–47]. On the theoretical side, the picture is equally open with estimates varying in an even larger range of thermal conductivity values between 25 and 20,000 W/m K [48,49,40,50–55]. This clearly shows great disagreements in the reported results of graphene thermal conductivity in the literature.

The aim of this investigation is to analyze the discrepancies in the reported thermal conductivity of graphene using different experimental and theoretical techniques. Also, the accuracy of the initially reported thermal conductivity in the literature will be discussed.

2. Experimental methods of measuring thermal conductivity of graphene

Various experimental techniques were used in the literature to measure the thermal conductivity of graphene such as Raman spectroscopy, microelectrothermal system, and scanning thermal microscopy. In what follows, we will elucidate the discrepancies in the measured results of thermal conductivity of graphene.

2.1. Raman spectroscopy

Raman spectroscopy of graphene has received considerable attention since the discovery of graphene [56,57]. Chen et al. [56] measured the thermal conductivity of a graphene monolayer grown by chemical vapor deposition and suspended over holes with different diameters using micro-Raman spectroscopy. The obtained thermal conductivity values of the suspended graphene ranged from (2.6 ± 0.9) to $(3.1 \pm 1.0) \times 10^3$ W/m K near 350 K without showing the sample size dependence predicted for suspended, clean, and flat graphene crystal. Lee et al. [37] measured the thermal conductivity of suspended single-layer graphene as a function of temperature using Raman scattering spectroscopy on clean samples prepared directly on a pre-patterned substrate by mechanical exfoliation without chemical treatments. Thermal conductivity was deduced by analyzing the heat diffusion equation assuming that the substrate is a heat sink at an ambient temperature. The obtained thermal conductivity values range from ~1800 W/m K near 325 K to ~710 W/m K at 500 K. Cai et al. [6] measured room-temperature thermal conductivity of $(370 + 650/-320)$ W/m K for the supported graphene. The thermal conductivity of the suspended graphene exceeds $(2500 + 1100/-1050)$ W/m K near 350 K and becomes $(1400 + 500/-480)$ W/m K at about 500 K. Jauregui et al. [57] conducted an experimental study to determine the thermal conductivity of graphene using Raman spectroscopy. The thermal conductivity of suspended CVD graphene was in the range of 1500–5000 W/m K using Raman spectroscopy.

Table 1 illustrates measured thermal conductivity values of graphene for various conditions using Raman spectroscopy method. It can be seen from this table that there is large discrepancies in the measured thermal conductivity results. For example, Balandin et al. [12] reported a value of 4840–5300 W/m K for graphene at room temperature, which seems to be substantially higher than those measured by a number of other investigators. On the other hand, Faugeras et al. [11] reported thermal conductivity of 632 W/m K at 660 K for exfoliated graphene which is close to the results reported by Lee et al. [37] at 500 K (~710 W/m K). The most important difference between the analysis of Balandin et al. [12] and the work of Lee et al. [37] and others is the value of the absorptance α of single layer graphene. Balandin et al. [12] used $\alpha = 13\%$, which is several times larger than the value of 2.3% measured and theoretically analyzed by Nair et al. [58]. If one uses $\alpha = 2.3\%$, their thermal conductivity value would reduce to 940 W/m K. Chen et al. [56] measured the thermal conductivity of a graphene monolayer grown by chemical vapor deposition and suspended over holes with different diameters ranging from 2.9 to 9.7 μm measured in vacuum using Raman spectroscopy. The obtained thermal conductivity values of the suspended graphene was ranging from (2.6 ± 0.9) to $(3.1 \pm 1.0) \times 10^3$ W/m K near 350 K.

Table 1 also demonstrates disagreements in the results associated with the effect of sample size on the thermal conductivity of graphene. For example, Ghosh et al. [36] and Balandin et al. [12] showed that as the diameter of the sample increases, the thermal conductivity increases. However, Chen et al. [56] illustrated that the thermal conductivity of graphene does not depend on the size of the sample. The results presented by Lee et al. [37] confirmed this finding. Fig. 1 demonstrates a wide dispersion of thermal conductivity of single layer graphene across various sample size using Raman Spectroscopy technique at room temperature. The sample size appears not correlating with thermal conductivity results of graphene. Therefore, this area of research would benefit from further studies which adhere to standard set of parameters to produce precise estimate of thermal conductivity of graphene. Lee et al. [37] showed that the thermal conductivity of graphene is strongly temperature dependent. As the temperature increases, the thermal conductivity of graphene decreases using the Raman Spectroscopy method. Using results from different studies in the literature, Fig. 2 illustrates the effect of varying the temperature on the thermal conductivity of single layer graphene using Raman spectroscopy. This figure clearly shows that as the temperature increases, the thermal conductivity of graphene decreases.

2.2. Microelectrothermal systems

Microelectrothermal systems have been used in recent years to measure the thermal conductivity of graphene [38,5,41–43,64,65]. Seol et al. [41] developed a nanofabricated resistance thermometer device to measure the thermal conductivity of graphene monolayers exfoliated onto silicon dioxide. The measurement results indicated that the thermal conductivity of the supported graphene was approximately 600 W/m K at room temperature. Dorgan et al. [42] studied the intrinsic transport properties of suspended graphene devices at high potential gradient fields and high temperatures ($\geqslant$1000 K). Their results revealed that the thermal conductivity of graphene was 2500 W/m K at room temperature and 310 W/m K at 1000 K. Bae et al. [64] illustrated experimentally a decrease of the thermal conductivity as the width reduced to a size regime comparable to the intrinsic phonon mean free path. For instance, at room temperature, thermal conductivity ~230, 170, 100, and 80 W/m K was observed for graphene nanoribbons (GNRs) of width ~130, 85, 65, and 45 nm, respectively. Xu et al. [40] reported measurements of thermal conduction in suspended single layer graphene (SLG) grown by chemical vapor deposition

Table 1
Thermal conductivity of graphene for various conditions using Raman spectroscopy method.

Layers	Refs.	Preparation process	Suspended/supported	Shape	Sample size μm	Laser wavelength nm	Temp. K	K (W/(m K))
Experimental data								
Raman spectroscopy								
SLG	[12]	Exfoliation	Suspended	Trench	2–5	488	RT	4840–5300
	[36]	Exfoliation	Suspended	Trench	1–5	488	RT	3080–5150
	[37]	Exfoliation	Suspended	Circular	2.3–3.6	514.5	325	~1800
					4.6–6.6		500	~710
	[11]	CVD	Suspended	Circular	44	632.8	660	~600
	[6]	CVD	Supported	Circular	3.8	532	350	2500+1100/−1050
							500	1400+500/−480
					2.9			~2500
					3.9			~2350
	[56]	CVD	Suspended	Circular	5	532	350	~2600
					8			~2950
					9.7			~2700
					9.7			~3100 (air)
	[59]	CVD	Suspended	Circular	2.8	538	300	4419
	[8]	CVD	Suspended	Circular	2.8	532	420	1875 (wrinkle free)
								1482 (wrinkled)
	[60]	CVD	Suspended	Fine structure			RT	100–1000
1					W: 5–16	488	RT	4100
2					L: 1–5			2800
3	[61]	Exfoliation	Suspended	Trench				2300
4								1400
8								1300
SLG					2.8	488	310	2778 ± 569
AB-BLG	[62]	CVD	Suspended	Circular			314	1896 ± 410
T-BLG							332	1413 ± 390
MLG	[63]	Sonication	Suspended	Trench	0.4–1	473	RT	340 (without annealing)
					T: 20 nm			560 (annealing)
FLG	[57]	CVD + exfoliation	Suspended	Trench	L: 20 μm W: 13 mm	532	RT	1500–5000

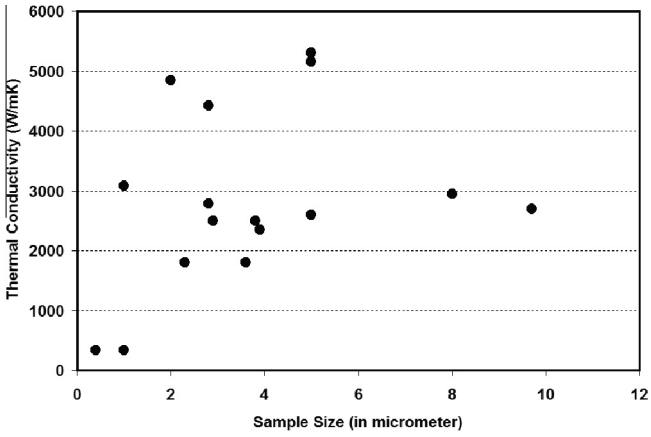

Fig. 1. Effect of the sample size on the thermal conductivity of graphene cited in many studies using Raman Spectroscopy method based on the works in Refs. [12,36,37,56,59,62,63].

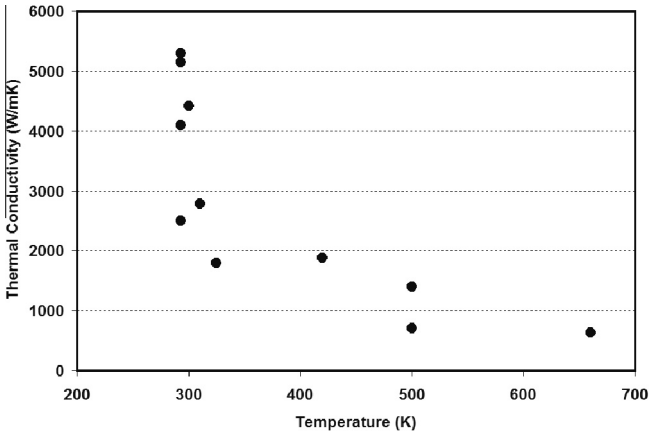

Fig. 2. Effect of the temperature on the thermal conductivity of graphene cited in many studies using Raman Spectroscopy method based on the works in Refs. [11,12,36,37,6,59,8,61,62].

on copper (Cu-CVD). The thermal conductivity at $T = 300$ K in the longest sample ($L = 9$ μm) exhibited a value of (1689 ± 100) W/m K ~ (1813 ± 111) W/m K. Table 2 illustrates different values of thermal conductivity of graphene measured at various conditions. This table clearly shows significant differences between results measured using Microelectrothermal method and Raman Spectroscopy.

2.3. Scanning thermal microscopy

Scanning thermal microscopy (SThM) has been used in the literature to measure the thermal conductivity of graphene [44–47]. Yoon et al. [44] measured thermal conductivity of residue-free suspended graphene bridge using null point scanning thermal conductivity. The thermal conductivity values of graphene, whose length and width were 3.6 and 5.52 μm, respectively, were measured as 2430 ± 190 W/m K, 2150 ± 170 W/m K, and 2100 ± 160 W/m K at the peak temperatures of 335 K, 361 K, and 366 K, respectively. Yu et al. [45] investigated the temperature distributions of Joule self-heated graphene nanoribbons (GNRs) with a spatial resolution finer than 100 nm by scanning thermal microscopy. The authors estimated an upper bound of the thermal conductivity of GNR as ~3800 W/m K. Pumarol et al. [46] reported direct imaging of nanoscale thermal transport in single and few-layer graphene (1, 3, 5, and 17 layers) with approximately 50 nm lateral resolution using high vacuum scanning thermal microscopy. The authors in a later study observed a decrease in thermal conductance of supported graphene with an increase in the number of layers. The measured results of thermal conductivity were approximately 920 W/m K, 317 W/m K, 205 W/m K, and

Table 2
Thermal conductivity of graphene for various conditions using microelectrothermal system.

Layers	Refs.	Preparation Process	Suspended/ supported	Shape	Sample size μm	Structure	Temp. K	K (W/(m K))
Experimental data								
Microelectrothermal system								
SLG	[38]	Exfoliation	Suspended	T	3 * 5	4-Probs	RT	2500
	[39]	Exfoliation	Suspended	T	3 * 0.5	Microresistance thermometer	280 <140	190 K–$T^{1.5}$
	[40]	CVD	Suspended	T	9 * 1.5	Microresistance thermometer	RT	~1700
	[5]	Exfoliation	Supported	T	9.5–12.5 1.5–3.2	Microresistance thermometer	RT	~600
	[41]	Exfoliation	Supported	T	3 * 12.5	Microresistance thermometer	RT	~600
	[42]	Exfoliation CVD	Suspended	T	0.85 * 1.5	Microresistance thermometer	RT 1000	~2500 (anneal & vaccum) ~310 (anneal & vaccum)
	[43]	CVD	Suspended	T	w: 170 w: 385 w: 120 w: 40	Electro-thermal micro-bridge	300	240 400 1700 2200
	[64]	Exfoliation	Supported	T	w: 17 w: 0.13 w: 0.085 w: 0.065 w: 0.045	Heat spreader	RT	320 (anneal) 230 (anneal) 170 (anneal) 100 (anneal) 80 (anneal)
1	[65]	Exfoliation	encased within SiO_2	T	Sensors W: 140 & 240	Heat spreader	310	~50 (anneal)
3								~100 (anneal)
10								~300 (anneal)
20								~1000 (anneal)
BLG	[66]	Exfoliation	Suspended	T	5 * 1.8	Microresistance thermometer	RT <125	~600 (anneal) K–$T^{1.5}$
BLG	[67]	Exfoliation	Suspended	T	7.5 * 5	Electro-thermal micro-bridge	RT	~900
2	[68]	Exfoliation	Suspended	T	3 * 5	T-bridge	RT	389 (without annealing)
3								344 (annealing)
4								302 (without annealing)
8								596 (annealing)
2	[69]	Exfoliation	Supported	T		Electrical self-heating	300	~630
6								~710
8								~810
27								~810
34								~950
2	[70]	Exfoliation	Supported	T		Electrical self-heating	RT	640
8								775
3	[71]	Exfoliation	Supported	T	5 * 5	Microresistance thermometer	RT	1250 (vaccum)
3			Supported		5 * 2	thermal-bridge		327 (vaccum)
3			Supported		5 * 1			150 (vaccum)
MLG			Suspended		5 * 1			170 (vaccum)
FLG	[66]	CVD	3D FOAM	T		Microresistance thermometer	RT	250 650 650 (annealing) 1600 (annealing) 650 (annealing) 650 (annealing)
FLG	[72]	CVD ribbons	Supported	T	0.2–1 * 0.016–0.052	Resistance thermometer	RT	1000–1400
FLG	[73]	CVD ribbons	Supported	T	0.2–0.7 * 0.016–0.09	Resistance thermometer	293 873	80 130
FLG	[74]	CVD-sheet Nano-ribbons	suspended	T	508 * 385	Electrical self-heating	198 873	126 (vaccum) 877 (vaccum)
FLG	[75]	CVD ribbons	suspended	T	0.846 * 0.169	Electro-thermal micro-bridge	80 300 380	~12.7 349 932
FLG	[76]	Reduced graphene oxide flakes	Supported Suspended Suspended	T	0.5 * 3	Electrical four-point	RT	2.87 0.14 0.87

65 W/m K for 1, 3, 5, and 17 layers respectively. Table 4 summarizes some of the thermal conductivity measurements of graphene using scanning thermal microscopy. Similar to the values obtained by Microelectro thermal measurements in Table 3, one can notice from this table that much smaller values of thermal conductivity of graphene are again observed here as well.

2.4. Theoretical models

The molecular dynamics simulation, which is a method for studying the physical movements of atoms and molecules, is used to determine the thermal conductivity of graphene [77–89]. For example, Nika et al. [77] suggested a simple model for the lattice

Table 3
Thermal conductivity of graphene for various conditions using scanning thermal microscopy.

Layers	Refs.	Preparation process	Suspended/ supported	Shape	Sample size (μm)	Description	Temp. (K)	K (W/(m K))
Experimental data								
Scanning thermal microscopy								
SLG	[44]	CVD + PDMS stamping	Suspended	T	3.6 * 5.52	Electrically heated +50 nm spatial resolution	335 361 366	2430 ± 190 2150 ± 170 2100 ± 160 (vacuum + no residue)
	[45]	Exfoliation	Suspended	T	0.086 * 3	Joule self-heated + 100 nm spatial resolution	RT	~3800 (vacuum + no residue)
1 3 5 17	[46]	Exfoliation	Suspended	T	W: 0.18	Joule self-heated + 50nm spatial resolution	RT	~920 ~317 ~205 ~65 (high vacuum + no residue)
FLG flake	[47]	Exfoliation	Suspended	–	–	Joule self-heated + 50nm spatial resolution	RT	~10 ~780–850 (vacuum)

thermal conductivity of graphene in the framework of Klemens approximation. They illustrated that the calculated thermal conductivity varied in the range of 1000–8000 W/m K. Munoz et al. [83] presented analytical expressions for the ballistic thermal conductance of a ribbon of limited width, approximating its phonon spectra by the vibrational modes of an elastic shell. The authors reported that the thermal conductivity was obtained for lengths exceeding the average mean free path to a value of 3960 W/m K.

Several molecular dynamic simulations in the literature have exhibited contradictory results (25 W/m K–20,000 W/m K) [85,96,99,102]. Cao [88] studied heat transport in monolayer graphene sheet using non-equilibrium molecular dynamics simulations. It was shown that the thermal transport in monolayer graphene sheet exhibited a strong length dependence on thermal conductivity; reaching 2360 W/m K at 2.8 μm. Wei et al. [91] investigated the in-plane lattice thermal conductivities of a single layer and multilayer graphene films using non-equilibrium dynamics simulations. It was found in that study the thermal conductivity of a single layer graphene was higher than that of a multilayer graphene. The results of that study showed that the in-plane thermal conductivities of a single layer, two layers, three layers, five layers, and graphite at 300 K were ~870 W/m K, ~825 W/m K, ~800 W/m K, ~575 W/m K, and ~525 W/m K, respectively. Garg et al. [93] investigated the thermal conductivity of a single layer graphene sheet by using an embedded approach of molecular dynamics (MD) and soft computing method. The effect of temperature and Stone–Thrower–Wales (STW) defects on the thermal conductivity of graphene sheet was analyzed in that study using MD simulation. The thermal conductivity of zigzag graphene sheet obtained from MD simulations was in the range of 30–80 W/m K. Table 4 shows the theoretical values of thermal conductivity of graphene for various conditions. It is interesting to note that even for theoretical models, wide discrepancies can be found in the thermal conductivity results (25 W/m K–20,000 W/m K). Figs. 3 and 4 summarize the minimum and maximum values of the thermal conductivity of graphene. It clearly seen in these figures that there is a large disagreement in the results using different methods and therefore more experimental and analytical studies should be conducted to unify these results.

3. Discussion

Thermal transport in graphene material has attracted a lot of attention as an area of research because of the potential for thermal management applications. Several measurements of the thermal conductivity of suspended graphene reported an extraordinarily large thermal conductivity compared with the thermal conductivity of diamond. Here we have presented a critical investigation of the thermal conductivity results of graphene using different experimental techniques and theoretical models. The results of the current investigation expose major discrepancies and problems in the obtained values of the thermal conductivity of grapheme reported in the literature.

Many studies were conducted in the literature and measured a wide range of thermal conductivity as depicted in Tables 1–4. Moreover, the theoretical results also display broad variations in the thermal conductivity of graphene. The large variations in the reported thermal conductivity can be caused by large measurement uncertainties as well as variations in the graphene quality and processing conditions. In addition, it is known that when a single-layer graphene is supported on an amorphous material, the thermal conductivity is reduced to about 500–600 W/m K at room temperature as a result of scattering of graphene lattice waves by the substrate [5,115,116] and can be even lower for few layer graphene encased in an amorphous oxide [65]. Similarly, polymeric residue can contribute to a similar reduction in the thermal conductivity of suspended graphene to approximately 500–600 W/m K for a bilayer graphene.

Based on the tabulated results in Tables 1–4, the high values for the graphene thermal conductivity seem to be significantly overestimated. In addition, a large variation in the thermal conductivity of graphene was noticed from the reported results using different experimental and numerical methods (0.14 W/m K–20,000 W/m K) [76,85]. Sadeghi et al. [117] reported some drawbacks of the experimental techniques for measuring thermal conductivity of graphene. For example, the major source of uncertainty in the Raman-based technique exists in the very different values of optical absorbance used in different studies. In addition to the uncertainty in the optical absorbance, the presence of local non-equilibrium may cause errors in the thermal conductivity results obtained from a data analysis based on Fourier's law [118]. Furthermore, Raman peak positions and their temperature dependence can be affected by strains and impurity amount in graphene [119,120]. These issues can result in significant errors when measuring the thermal conductivity of graphene using the Raman technique. This raises a major concern on the accuracy of the experimental techniques that were used to measure the thermal conductivity of graphene at the nanoscale level. Thus, more pertinent studies need to be conducted to accurately report the thermal conductivity of graphene under various conditions.

When materials and devices are reduced to a sufficiently small size, the thermal, electrical, and optical characteristics become clearly different from those at the macroscale and nanoscale. Microscale heat transfer becomes significant when the mean free path of the heat carrier becomes comparable to the characteristic length of the device and the continuum approach becomes invalid at this length scale. Tien and Chen [121] addressed challenges in

Table 4
Thermal conductivity of graphene using theoretical models for various conditions.

Layers	Ref.	Method	Description	K (W/(m K))
Theoretical data				
SLG	[77]	BTE,γ_{LA},γ_{TA}	Strong size dependence	1000–8000
	[78]	BTE,$\gamma_s(q)$	Depends on the flake width, defect concentration and roughness of the edges	2000–5000
	[79]	BTE	K (graphene) $\geqslant$ K (carbon nanotube)	~2430
	[80]	BTE	Weak interlayer coupling	1500–3500
	[81]	BTE	Strong dimension dependence	100–8000
	[82]	Semi-continuum model	Depends on the tensile and compression strain, defects amount, and isotope concentration	2000–4000
	[83]	Ballistic elastic-shell-based theory	Strong width dependence	3960
	[84]	MD simulation	Depends on the vacancy defect concentrations	2903 ± 93
	[85]	Valence force field model (VFFM)	Ballistic region	20,000
	[86]	Non-equilibrium MD simulation	Strong length and defect density dependence	100 to ~550
	[87]	MD simulation	Length ~16 μm, strong length dependence	3200
	[88]	MD simulation	Strong length dependence	2360
	[89]	MD simulation	Strong strain dependence	~3500 to ~5500
	[90]	MD simulation and relaxation time approximation (RTA) method	Isolated size 60 × 60 Å	1779.7
	[90]	MD simulation and relaxation time approximation (RTA) method	60x60 Å sheet; Cu—supported; dependents on the interaction strength between graphene and substrate	1281.5
	[91]	MD simulation	Length (7–25 nm), strong bonding strength dependence	~870
	[92]	MD simulation	Strong defect concentration dependence	1720 (No defects) ~100–180 (with defects)
	[93]	MD simulation	Strong defect concentration dependence	30–80
	[94]	MD + finite element modeling	Strong dependence on the grain boundary contact resistance and grain size	–
	[95]	BTE	L ~10 μm; Strong dependence on the direction of acoustic, isotopic percentages, temperature and L; insensitive to strain.	800–3500
	[50]	BTE	Strong dependence on the isotopic percentages, temperature and L	500–5000
	[40]	MD simulation	L: 300 nm ~9 μm; dependence on the temperature and sample length	50–2300
	[96]	MD simulation	L: 20.5 nm Dependence on the geometric variation of doped boron and temperature	~25–80
	[48]	MD simulation	$k(r_G) = k_{c\text{-}Graph}/(1 + R_{GB}{}^{*}k_{c\text{-}Graph}/2r_G)$; $k(c_{GB}) = k_{c\text{-}Graph}/(1 + c_{GB}{}^{*}R_{GB}{}^{*}k_{c\text{-}Graph}/d_l)$	~24–860
	[97]	BTE + MD	Temperature-dependent; length-dependent; width-dependent	<1000
	[98]	MD simulation	Strong dependence on carbonyl pairs and vacancies lead; Weak dependence on hydroxyl, epoxy groups and nano-holes	~60–3500
	[99]	BTE	L: 3, 10, 100 μm; Dependence on Length, temperature, LA, TA and ZA	~600–8000
	[49]	First principles BPE	Size-dependent and stain-dependent when sample larger than 500 μm; temperature-dependent	<20,000
FLG	[61]	BTE,$\gamma_s(q)$	$n = 8 - 1$, strong size dependence	1000–4000
	[80]	BTE	$n = 5 - 1$, strong size dependence	1000–3500
	[100]	Linearized Boltzmann transport equation and perturbation theory	$n = 4 - 1$	2000–3300
	[91]	MD simulation	$n = 5 - 1$, strong dependence on the bonding strength	580–880
	[101]	Semi-continuum model	$n = 10 - 1$, strong dependence on the number of layers, temperature and L_c	~2700–5000
GNRs 7000 ~ 20,000	[102]	MD simulation	Strong function of the ribbon width Graphene sheet size: ~20 A	~500–
	[103]	BTE + Full phonon dispersions	Depend strongly on the width of the nanoribbon and the rms height of the edge roughness	~5500
	[4]	MD simulation	At 400 K for a 1.5 nm × 5.7 nm zigzag GNR), Depends on vacancies and edge roughness in the nanoribbons	~2000
	[104,105]	AIREBO potential + MD simulation	Strong defect density dependence	30–80
	[106]	MD simulation	Extremely sensitive to defect configuration; strong length dependance	3000–5200
	[107]	MD simulation	$K \sim L^{0.24}$, 100 nm $\leqslant L \leqslant$ 650 nm	400–600
	[108]	MD simulation	10 nm*2.1 nm; Strong tensile strain dependence; insensitive to compressive strain	~75
	[109]	MD simulation	2 nm*11 nm; dependence on N shape doping, N atom doping concentration	20–95
	[51]	MD simulation	Dependence on the edge effects	70–100
	[52]	MD simulation	50 nm*4.26 nm; Strong dependence on the isotopic percentages	-
	[53]	MD simulation	20–110 nm*4.26 nm; dependence on the length and isotopic	~86–215
	[54]	Direction-dependent phonon-boundary scattering + BTE	L: 10 μm; W: 0.5,1.0,5.0 μm; Dependence on the effects of size and temperature , LA, TA and ZA branches	~250–7000
	[55]	MD simulation	ZGNRs have better torsional rigidity than AGNRs; The thermal conductivity of length-fixing GNRs decreases with the increase of torsional deformation and temperature; The wider GNRs have better anti-torsion capability and thermal conductivity	~50–500
	[110]	BTE	W < 1.5 μm , weak width-dependent; MFPs > 1 μm, strong long MFP phonons-dependent	~2000
	[111]	BTE	Dependence on length, width, temperature and roughness	<6000
GNRs on SiO_2	[112]	BTE	Strong edge and width dependence	100–1000
FlGNRs	[113]	MD simulation	10-ZGNR, $n = 1,\ldots, 5$	300–500
FLGNRs on SiO_2	[114]	MD simulation	Dependence on the equivalent molecule number density(ρ) and Number of molecules(N)	520–700

the field of micro-length scale radiative and conductive heat transfer in solids. A number of experimental works have reported a reduced thermal conductivity at the microscale [120,122]. Yu et al. [122] investigated the temperature dependence of aluminum gallium arsenide (GaAs/AlAs) thin film structures. Their results demonstrated that the thermal conductivity/diffusivity of the

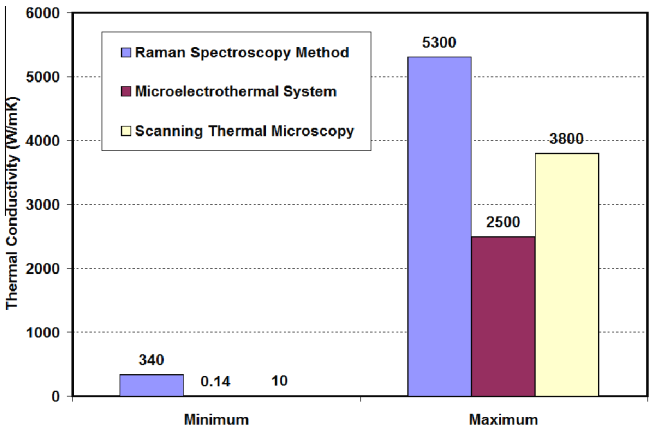

Fig. 3. Variation of thermal conductivity of graphene using different experimental methods based on the works in Refs. [12,63,76,42,45,47].

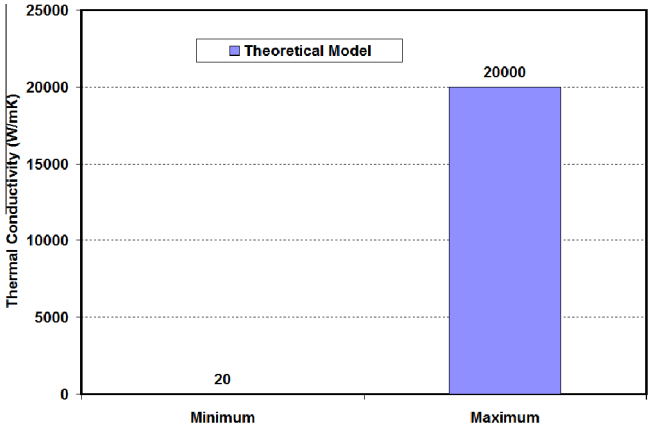

Fig. 4. Variation of thermal conductivity of graphene using theoretical model based on the works in Refs. [85,102,109].

structure were lower than its corresponding bulk values. The temperature dependence of its thermophysical properties was weaker than that of the typical bulk materials. Interface scattering was believed to be the major cause of the observed reduction in the thermal conductivity.

Chen et al. [120] developed a measurement technique that determined the thermal diffusivity of thin films in both parallel and perpendicular directions, and presented experimental results on the thermal diffusivity of GaAs/AlGaAs-based thin-film structures. The results demonstrated that the thermal diffusivity of the vertical-cavity surface-emitting laser (VCSEL) structure was 5–7 times smaller than that of its corresponding bulk media. The authors attributed this large difference to the anisotropy of thermal diffusivity caused solely by the effects of interfaces and boundaries of the thin film. Contrary to the prior analyzed results, the above examples actually show deterioration in the thermal properties as compared to bulk properties. Piprek [123] presented direct thermal conductivity measurements of separated GaAs–AlAs DBRs (distributed Bragg reflectors) with a quarter-wave layer thickness of more than 100 nm. Using an ac calorimetric method and finite element analysis, a 50% thermal conductivity reduction was found compared to the average bulk value.

It should be noted that the thermal conductivity is a macro manifestation of a measure that shows a substance's ability to transfer the heat. As such the measurement of the ability of a single layer of carbon atoms to carry the heat itself comes into question. The huge disparities in the obtained values for the thermal conductivity of Graphene further aggravates the problem. Understanding energy transport mechanisms at the micro- and nano-scale becomes increasingly important. This requires accurate investigation of material properties, along with the development of new technologies to characterize energy transfer at these scales.

4. Conclusions

A comprehensive synthesis of the thermal conductivity of a single layer graphene (SLG), few layer graphene (FLG), multiple-layer graphene (MLG), and nanoribbons graphene (NRG) was presented in this work. The results of different experimental and theoretical techniques were summarized in Tables 1–4 for various conditions such as preparation process, shape, sample size, wavelength, and temperature. Wide variations in the thermal conductivity results were reported in different studies. The initially measured thermal conductivity appears to be considerably overestimated. Majority of the cited studies subsequently reported lower values of thermal conductivity than the earlier published results. Moreover, significant inconsistency in the results were noticed in the results of the thermal conductivity of graphene using various experimental and theoretical techniques (0.14 W/m K–20,000 W/m K). Most of the experimental methods unanimously illustrated the dependence of graphene thermal conductivity results on temperature. Raman spectroscopy illustrated that the thermal conductivity of graphene decreases with an increase in the temperature. Disagreement was also reported on the effect of sample size on the thermal conductivity results of graphene. The initially reported results showed sample size dependence while the subsequent studies illustrated insignificant effect of the sample size. Thus, more experimental and theoretical studies should be conducted to accurately determine the thermal conductivity of graphene.

References

[1] A.K. Geim, P. Kim, Carbon wonderland, Sci. Am. 298 (2008) 90–97.
[2] A.K. Geim, K.S. Novoselov, The rise of graphene, Nat. Mater. 6 (2007) 183–191.
[3] A.H. Castro Neto, F. Guinea, N.M.R. Peres, K.S. Novoselov, A.K. Geim, The electronic properties of graphene, Rev. Mod. Phys. 81 (2009) 109–162.
[4] J. Hu, X. Ruan, Y.P. Chen, Thermal conductivity and thermal rectification in graphene nanoribbons: a molecular dynamics study, Nano Lett. 9 (2009) 2730–2735.
[5] Jae Hun Seol, Insun Jo, Arden L. Moore, Lucas Lindsay, Zachary H. Aitken, Michael T. Pettes, Xuesong Li, Zhen Yao, Rui Huang, David Broido, Natalio Mingo, Rodney S. Ruoff, Li Shi, Two-dimensional phonon transport in supported graphene, Science 328 (2010) 213–216.
[6] W. Cai, A.L. Moore, Y. Zhu, X. Li, S. Chen, L. Shi, R.S. Ruoff, Thermal transport in suspended and supported monolayer graphene grown by chemical vapor deposition, Nano Lett. 10 (2010) 1645–1651.
[7] S. Chen, Qingzhi Wu, Columbia Mishra, Junyong Kang, Hengji Zhang, Kyeongjae Cho, Weiwei Cai, Alexander A. Balandin, Rodney S. Ruoff, Thermal conductivity of isotopically modified graphene, Nat. Mater. 11 (2012) 203–207.
[8] S. Chen, Qiongyu Li, Qimin Zhang, Yan Qu, Hengxing Ji, Rodney S. Ruoff, Weiwei Cai, Thermal conductivity measurements of suspended graphene with and without wrinkles by micro-Raman mapping, Nanotechnology 23 (2012) 365701.
[9] T.Y. Kim, C.-H. Park, N. Marzari, The electronic thermal conductivity of graphene, Nano Lett. 16 (2016) 2439–2443.
[10] E. Pop, V. Varshney, A.K. Roy, Thermal properties of graphene: fundamentals and applications, MRS Bull. 37 (2012) 1273–1281.
[11] C. Faugeras, B. Faugeras, M. Orlita, M. Potemski, R.R. Nair, A.K. Geim, Thermal conductivity of graphene in corbino membrane geometry, ACS Nano 4 (2010) 1889–1892.
[12] A.A. Balandin, S. Ghosh, W. Bao, I. Calizo, D. Teweldebrhan, F. Miao, C.N. Lau, Superior thermal conductivity of single-layer graphene, Nano Lett. 8 (2008) 902–907.
[13] K. Vafai, N. Zhu, On the analysis of asymmetric disk-shaped and flat-plate heat pipes, ASME J. Heat Transfer 136 (2014) 116001-1–116001-2, http://dx.doi.org/10.1115/1.4028430.
[14] K. Alizad, K. Vafai, M. Shafahi, Thermal performance and operational attributes of the startup characteristics of flat-shaped heat pipes using nanofluids, Int. J. Heat Mass Transf. (2011), http://dx.doi.org/10.1016/j.ijheatmasstransfer.2011.08.050.

[15] M. Shafahi, V. Bianco, K. Vafai, O. Manca, Thermal performance of flat-shaped heat pipes using nanofluids, Int. J. Heat Mass Transf. 53 (2010) 1438–1445.
[16] M. Shafahi, V. Bianco, K. Vafai, O. Manca, An investigation of the thermal performance of cylindrical heat pipes using nanofluids, Int. J. Heat Mass Transf. 53 (2010) 376–383.
[17] Y. Wang, K. Vafai, An experimental investigation of the transient characteristics on a flat-plate heat pipe during startup and shutdown operations, ASME J. Heat Transfer 122 (2000) 525–535.
[18] Y. Wang, K. Vafai, An experimental investigation of the thermal performance of an asymmetrical flat plate heat pipe, Int. J. Heat Mass Transf. 43 (2000) 2657–2668.
[19] Y. Wang, K. Vafai, Transient characterization of flat plate heat pipes during startup and shutdown operations, Int. J. Heat Mass Transf. 43 (2000) 2641–2655.
[20] N. Zhu, K. Vafai, Analysis of cylindrical heat pipes incorporating the effects of liquid–vapor coupling and non-Darcian transport – a closed form solution, Int. J. Heat Mass Transf. 42 (1999) 3405–3418.
[21] N. Zhu, K. Vafai, Analytical modeling of the startup characteristics of asymmetrical flat-plate and disk-shaped heat pipes, Int. J. Heat Mass Transf. 41 (1998) 2619–2637.
[22] N. Zhu, K. Vafai, Vapor and liquid flow in an asymmetrical flat plate heat pipe-a three dimensional analytical and numerical investigation, Int. J. Heat Mass Transf. 41 (1998) 159–174.
[23] N. Zhu, K. Vafai, Numerical and analytical investigation of vapor flow in a disk-shaped heat pipe incorporating secondary flow, Int. J. Heat Mass Transf. 40 (1997) 2887–2900.
[24] N. Zhu, K. Vafai, The effects of liquid-vapor coupling and non-Darcian transport on asymmetrical disk-shaped heat pipes, Int. J. Heat Mass Transf. 39 (1996) 2095–2113.
[25] N. Zhu, K. Vafai, Optimization of asymmetrical disk-shaped heat pipes, AIAA J. Thermophys. Heat Transfer 10 (1996) 179–182.
[26] K. Vafai, N. Zhu, W. Wang, Analysis of asymmetric disk-shaped and flat plate heat pipes, ASME J. Heat Transfer 117 (1995) 209–218.
[27] K. Vafai, W. Wang, Analysis of flow and heat transfer characteristics of an asymmetrical flat plate heat pipe, Int. J. Heat Mass Transf. 35 (1992) 2087–2099.
[28] A.R.A. Khaled, K. Vafai, Cooling augmentation using microchannels with rotatable separating plates, Int. J. Heat Mass Transf. 54 (2011) 3732–3739.
[29] K. Vafai, A.-R.A. Khaled, Analysis of flexible microchannel heat sink systems, Int. J. Heat Mass Transf. 48 (2005) 1739–1746.
[30] D.Y. Lee, K. Vafai, Comparative analysis of jet impingement and microchannel cooling for high heat flux applications, Int. J. Heat Mass Transf. 42 (1999) 1555–1568.
[31] L. Ma, J. Wang, F. Ding, Recent progress and challenges in graphene nanoribbon synthesis, ChemPhysChem 14 (2013) 47–54.
[32] W. Choi, I. Lahiri, R. Seelaboyina, Y.S. Kang, Synthesis of graphene and its applications: a review, Crit. Rev. Solid State Mater. Sci. 35 (2010) 52–71.
[33] S. Das Sarma, S. Adam, E.H. Hwang, E. Rossi, Electronic transport in two-dimensional graphene, Rev. Mod. Phys. 83 (2011) 407–470.
[34] X. Zhang, J. Xin, F. Ding, The edges of graphene, Nanoscale 5 (2013) 2556–2569.
[35] J.D. Renteria, D.L. Nika, A.A. Balandin, Graphene thermal properties: applications in thermal management and energy storage, Appl. Sci. 4 (2014) 525–547.
[36] S. Ghosh, I. Calizo, D. Teweldebrhan, E.P. Pokatilov, D.L. Nika, A.A. Balandin, W. Bao, F. Miao, C.N. Lau, Extremely high thermal conductivity of graphene: prospects for thermal management applications in nanoelectronic circuits, Appl. Phys. Lett. 92 (2008) 151911.
[37] Jae-Ung Lee, Duhee Yoon, Hakseong Kim, Sang Wook Lee, Hyeonsik Cheong, Thermal conductivity of suspended pristine graphene measured by Raman spectroscopy, Phys. Rev. B. 83 (2011) 081419.
[38] Jaehyun Kim, Eric Ou, Daniel P. Sellan, Li Shi, A four-probe thermal transport measurement method for nanostructures, Rev. Sci. Instrum. 86 (2015) 044901.
[39] Xiangfan Xu, Yu Wang, Kaiwen Zhang, Xiangming Zhao, Sukang Bae, Martin Heinrich, Cong Tinh Bui, Rongguo Xie, John T.L. Thong, Byung Hee Hong, Kian Ping Loh, Baowen Li, Barbaros Ozyilmaz, Phonon transport in suspended single layer graphene, Preprint at arXiv:org/abs/1012.2937 (abstract) and arXiv:org/pdf/1012.2937.pdf (full paper), 2010.
[40] Xiangfan Xu, Luiz F.C. Pereira, Yu Wang, Jing Wu, Zhang Kaiwen, Xiangming Zhao, Sukang Bae, Cong Tinh Bui, Rongguo Xie, John T.L. Thong, Byung Hee Hong, Kian Ping Loh, Davide Donadio, Baowen Li, Barbaros Ozyilmaz, Length-dependent thermal conductivity in suspended single-layer graphene, Nat. Commun. 5 (2014) 3689.
[41] Jae Hun Seol, Arden L. Moore, Li Shi, Insun Jo, Zhen Yao, Thermal conductivity measurement of graphene exfoliated on silicon dioxide, J. Heat Transfer 133 (2011). 022403-1.
[42] Vincent E. Dorgan, Ashkan Behnam, Hiram J. Conley, Kirill I. Bolotin, Eric Pop, High-field electrical and thermal transport in suspended graphene, Nano Lett. 13 (2013) 4581–4586.
[43] Lifei Chen, Huaqing Xie, Wei Yu, Bingqian Wang, Zihua Wu, Thermal transport behaviors of suspended graphene sheets with different sizes, Int. J. Therm. Sci. 94 (2015) 221–227.
[44] Kichul Yoon, Gwangseok Hwangb, Jaehun Chungb, Hong goo Kim, Ohmyoung Kwon, Kenneth David Kihm, Joon Sik Lee, Measuring the thermal conductivity of residue-free suspended graphene bridge using null point scanning thermal microscopy, Carbon 76 (2014) 77–78.
[45] Young-Jun Yu, Melinda Y. Han, Stéphane Berciaud, Alexandru B. Georgescu, Tony F. Heinz, Louis E. Brus, Kwang S. Kim, Philip Kim, High-resolution spatial mapping of the temperature distribution of a Joule self-heated graphene nanoribbon, Appl. Phys. Lett. 99 (2011) 183105.
[46] Manuel E. Pumarol, Mark C. Rosamond, Peter Tovee, Michael C. Petty, Dagou A. Zeze, Vladimir Falko, Oleg V. Kolosov, Direct nanoscale imaging of ballistic and diffusive thermal transport in graphene nanostructures, Nano Lett. 12 (2012) 2906–2911.
[47] Fabian Menges, Heike Riel, Andreas Stemmer, Christos Dimitrakopoulos, Bernd Gotsmann, Thermal transport into graphene through nanoscopic contacts, Phys. Rev. Lett. 111 (2013) 205901.
[48] Konstanze R. Hahn, Claudio Melis, Luciano Colombo, Thermal transport in nanocrystalline graphene investigated by approach-to-equilibrium molecular dynamics simulations, arXiv:1507.08927v1 [cond-mat.mtrl-sci], 31 June 2015.
[49] Youdi Kuang, Lucas Lindsay, Sanqiang Shi, Xinjiang Wang, Ruiqiang Guo, Baoling Huang, Thermal conductivity of graphene mediated by strain and size, rXiv:1506.08380v1, 28 Jun 2015.
[50] Giorgia Fugallo, Andrea Cepellotti, Lorenzo Paulatto, Michele Lazzeri, Nicola Marzari, Francesco Mauri, Thermal conductivity of graphene and graphite: collective excitations and mean free paths, Nano Lett. 14 (2014) 6109–6114.
[51] Huisheng Zhang, Tong Zhou, Guofeng Xie, Juexian Cao, Zhongqin Yang, Thermal transport in folded zigzag and armchair graphene nanoribbons, Appl. Phys. Lett. 104 (2014) 241908.
[52] Scott Broderick, Upamanyu Ray, Srikant Srinivasan, Krishna Rajan, Ganesh Balasubramanian, An informatics based analysis of the impact of isotope substitution on phonon modes in graphene, Appl. Phys. Lett. 104 (2014) 243110.
[53] Upamanyu Ray, Ganesh Balasubramanian, Reduced thermal conductivity of isotope substituted carbon nanomaterials: nanotube versus graphene nanoribbon, Chem. Phys. Lett. 599 (2014) 154–158.
[54] Yulu Shen, Guofeng Xie, Xiaolin Wei, Kaiwang Zhang, Minghua Tang, Jianxin Zhong, Gang Zhang, YongWei Zhang, Size and boundary scattering controlled contribution of spectral phonons to the thermal conductivity in graphene ribbons, J. Appl. Phys. 115 (2014) 063507.
[55] Haijun Shen, Mechanical properties and thermal conductivity of the twisted graphene nanoribbons, Mol. Phys. 112 (2014) 2614–2620.
[56] S.S. Chen, A.L. Moore, W.W. Cai, J.W. Suk, J. An, C. Mishra, C. Amos, C.W. Magnuson, J. Kang, L. Shi, R.S. Ruoff, Raman measurements of thermal transport in suspended monolayer graphene of variable sizes in vacuum and gaseous environments, ACS Nano 5 (2011) 321–328.
[57] L.A. Jauregui, Y. Yue, A.N. Sidorov, J. Hu, Q. Yu, G. Lopez, R. Jalilian, D.K. Benjamin, D.A. Delk, W. Wu, et al., Thermal transport in graphene nanostructures: experiments and simulations, ECS Trans. 28 (2010) 73–83.
[58] R.R. Nair, P. Blake, A.N. Grigorenko, K.S. Novoselov, T.J. Booth, T. Stauber, N.M. R. Peres, A.K. Geim, Fine structure constant defines visual transparency of graphene, Science 320 (2008) 1308.
[59] S. Chen, Qingzhi Wu, Columbia Mishra, Junyong Kang, Hengji Zhang, Kyeongjae Cho, Weiwei Cai, Alexander A. Balandin, Rodney S. Ruoff, Thermal conductivity of isotopically modified graphene, Nat. Mater. 11 (2012) 203–207.
[60] I. Vlassiouk, S. Smirnov, I. Ivanov, P.F. Fulvio, S. Dai, H. Meyer, M. Chi, D. Hensley, P. Datskos, N.V. Lavrik, Electrical and thermal conductivity of low temperature CVD graphene: the effect of disorder, Nanotechnology 22 (2011) 275716.
[61] S. Ghosh, W. Bao, D.L. Nika, S. Subrina, E.P. Pokatilov, C.N. Lau, A.A. Balandin, Dimensional crossover of thermal transport in few-layer graphene, Nat Mater. 9 (2010) 555–558.
[62] Hongyang Li, Hao Ying, Xiangping Chen, Denis L. Nika, Alexandr I. Cocemasov, Weiwei Cai, Alexander A. Balandin, Shanshan Chen, Thermal conductivity of twisted bilayer graphene, Nanoscale 6 (2014) 13402–13408.
[63] Victor A. Ermakov, Andrei V. Alaferdov, Alfredo R. Vaz, Alexander V. Baranov, Stanislav A. Moshkalev, Nonlocal laser annealing to improve thermal contacts between multi-layer graphene and metals, Nanotechnology 24 (2013) 155301.
[64] Myung-Ho Bae, Zuanyi Li, Zlatan Aksamija, Pierre N. Martin, Feng Xiong, Zhun-Yong Ong, Irena Knezevic, Eric Pop, Ballistic to diffusive crossover of heat flow in graphene ribbons, Nat. Commun. 4 (2013) 1734.
[65] W. Jang, Z. Chen, W. Bao, C.N. Lau, C. Dames, Thickness-dependent thermal conductivity of encased graphene and ultrathin graphite, Nano Lett. 10 (2010) 3909–3913.
[66] Michael Thompson Pettes, Insun Jo, Zhen Yao, Li Shi, Influence of polymeric residue on the thermal conductivity of suspended bilayer graphene, Nano Lett. 11 (2011) 1195–1200.
[67] Insun Jo, Michael T. Pettes, Lucas Lindsay, Eric Ou, Annie Weathers, Arden L. Moore, Zhen Yao, Li Shi, Reexamination of basal plane thermal conductivity of suspended graphene samples measured by electro-thermal micro-bridge methods, AIP Adv. 5 (2015) 053206.
[68] W. Jang, W. Bao, L. Jing, C.N. Lau, C. Dames, Thermal conductivity of suspended few-layer graphene by a modified T-bridge method, Appl. Phys. Lett. 103 (2013) 133102.
[69] Mir Mohammad Sadeghia, Insun Joa, Li Shi, Phonon-interface scattering in multilayer graphene on an amorphous support, Appl. Phys. Sci. 110 (2013) 16323.
[70] M.M. Sadeghi, L. Shi, in: Proceedings of the 2011 ASME International Mechanical Engineering Congress and Exposition, Denver, Colorado, USA, 2011, pp. 64227.

[71] Ziqian Wang, Rongguo Xie, Cong Tinh Bui, Dan Liu, Xiaoxi Ni, Baowen Li, John T.L. Thong, Thermal transport in suspended and supported few-layer graphene, Nano Lett. 11 (2011) 113–118.
[72] R. Murali, Y. Yang, K. Brenner, T. Beck, J.D. Meindl, Breakdown current density of graphene nanoribbons, Appl. Phys. Lett. 94 (2009) 243114.
[73] A.D. Liao, J.Z. Wu, X. Wang, K. Tahy, D. Jena, H. Dai, E. Pop, Thermally limited current carrying ability of graphene nanoribbons, Phys. Rev. Lett. 106 (2011) 256801.
[74] Huaqing Xie, Lifei Chen, Wei Yu, Bingqian Wang, Temperature dependent thermal conductivity of a free-standing graphene nanoribbon, Appl. Phys. Lett. 102 (2013) 111911.
[75] Qin-Yi Li, Koji Takahashi, Hiroki Ago, Xing Zhang, Tatsuya Ikuta, Takashi Nishiyama, Kenji Kawahara, Temperature dependent thermal conductivity of a suspended submicron graphene Ribbon, J. Appl. Phys. 117 (2015) 065102.
[76] Timo Schwamb, Brian R. Burg, Niklas C. Schirmer, Dimos Poulikakos, An electrical method for the measurement of the thermal and electrical conductivity of reduced graphene oxide nanostructures, Nanotechnology 20 (2009) 405704.
[77] D.L. Nika, S. Ghosh, E.P. Pokatilov, A.A. Balandin, Lattice thermal conductivity of graphene flakes: comparison with bulk graphite, Appl. Phys. Lett. 94 (2009) 203103.
[78] D.L. Nika, E.P. Pokatilov, A.S. Askerov, A.A. Balandin, Phonon thermal conduction in graphene: role of Umklapp and edge roughness scattering, Phys. Rev. B 79 (2009) 155413.
[79] L. Lindsay, D.A. Broido, N. Mingo, Diameter dependence of carbon nanotube thermal conductivity and extension to the graphene limit, Phys. Rev. B 82 (2010) 161402.
[80] L. Lindsay, D.A. Broido, N. Mingo, Flexural phonons and thermal transport in multilayer graphene and graphite, Phys. Rev. B 83 (2011) 235428.
[81] D.L. Nika, A.S. Askerov, A.A. Balandin, Anomalous size dependence of the thermal conductivity of graphene ribbons, Nano Lett. 12 (2012) 3238–3244.
[82] A. Alofi, G.P. Srivastava, Thermal conductivity of graphene and graphite, Phys. Rev. B 87 (2013) 115421.
[83] E. Munoz, J. Lu, B.I. Yakobson, Ballistic thermal conductance of graphene ribbons, Nano Lett. 10 (2010) 1652–1656.
[84] H. Zhang, G. Lee, K. Cho, Thermal transport in graphene and effects of vacancies, Phys. Rev. B 84 (2011) 115460.
[85] J.-W. Jiang, J.-S. Wang, B. Li, Thermal conductance of graphite and dimerite, Phys. Rev. B 79 (2009) 205418.
[86] Y.Y. Zhang, Y. Cheng, Q.X. Pei, C.W. Wang, Y. Xiang, Thermal conductivity of defected graphene, Phys. Lett. A 376 (2012) 3668–3672.
[87] M. Park, S.C. Lee, Y.S. Kim, Length-dependent thermal conductivity of graphene and its macroscopic limit, J. Appl. Phys. 114 (2013) 053506.
[88] A. Cao, Molecular dynamics simulation study on heat transport in monolayer graphene sheet with various geometries, J. Appl. Phys. 111 (2012) 083528.
[89] F. Ma, H.B. Zheng, Y.J. Sun, D. Yang, K.W. Xu, P.K. Chu, Strain effect on lattice vibration, heat capacity, and thermal conductivity of graphene, Appl. Phys. Lett. 101 (2012) 111904.
[90] L. Cheng, S. Kumar, Thermal transport in graphene supported copper, J. Appl. Phys. 112 (2012) 043502.
[91] Zhiyong Wei, Zhonghua Ni, Kedong Bi, Minhua Chen, Yunfei Chen, In-plane lattice thermal conductivities of multilayer graphene films, Carbon 49 (2011) 2653–2658.
[92] N. Khosravian, M.K. Samani, G.C. Loh, G.C.K. Chen, D. Baillargeat, B.K. Tay, Effects of a grain boundary loop on the thermal conductivity of graphene: a molecular dynamics study, Comput. Mater. Sci. 79 (2013) 132–135.
[93] A. Garg, V. Vijayaraghavan, C.H. Wong, K. Tai, Liang Gao, An embedded simulation approach for modeling the thermal conductivity of 2D nanoscale material, Simul. Model. Pract. Theory 44 (2014) 1–13.
[94] Bohayra Mortazavi, Markus Pötschke, Gianaurelio Cuniberti, Multiscale modeling of thermal conductivity of polycrystalline graphene sheets, Nanoscale 6 (2014) 3344–3352.
[95] L. Lindsay, Wu Li, Jeśus Carrete, Natalio Mingo, D.A. Broido, T.L. Reinecke, Phonon thermal transport in strained and unstrained graphene from first principles, Phys. Rev. B 89 (2014) 155426.
[96] Qi Liang, Yuan Wei, Molecular dynamics study on the thermal conductivity and thermal rectification in graphene with geometric variations of doped boron, Phys. B 437 (2014) 36–40.
[97] Poya Yasaei, Arman Fathizadeh, Reza Hantehzadeh, Arnab K. Majee, Ahmed El-Ghandour, David Estrada, Craig Foster, Zlatan Aksamija, Fatemeh Khalili-Araghi, Amin Salehi-Khojin, Bimodal phonon scattering in graphene grain boundaries, Nano Lett. 15 (2015) 4532–4540.
[98] Weiwei Zhao, Yanlei Wang, Zhangting Wu, Wenhui Wang, Kedong Bi, Zheng Liang, Juekuan Yang, Yunfei Chen, Zhiping Xu, Zhenhua Ni, Defect-engineered heat transport in graphene: a route to high efficient thermal rectification, Nature (2015) 11962.
[99] Xiaokun Gu, Ronggui Yang, First-principles prediction of phononic thermal conductivity of silicene: a comparison with graphene, J. Appl. Phys. 117 (2015) 025102.
[100] D. Singh, J.Y. Murthy, T.S. Fisher, Mechanism of thermal conductivity reduction in few-layer graphene, J. Appl. Phys. 110 (2011) 044317.
[101] A. Alofi, G.P. Srivastava, Evolution of thermal properties from graphene to graphite, Appl. Phys. Lett. 104 (2014) 031903.
[102] W.J. Evans, L. Hu, P. Keblinsky, Thermal conductivity of graphene ribbons from equilibrium molecular dynamics: effect of ribbon width, edge roughness, and hydrogen termination, Appl. Phys. Lett. 96 (2010) 203112.
[103] Z. Aksamija, I. Knezevic, Lattice thermal conductivity of graphene nanoribbons: anisotropy and edge roughness scattering, Appl. Phys. Lett. 98 (2011) 141919.
[104] T. Ng, J.J. Yeo, Z.S. Liu, A molecular dynamics study of the thermal conductivity of graphene nanoribbons containing dispersed Stone–Thrower–Wales defects, Carbon 50 (2012) 4887–4893.
[105] J.J. Yeo, Z. Liu, T.Y. Ng, Comparing the effects of dispersed Stone–Thrower–Wales defects and double vacancies on the thermal conductivity of graphene nanoribbons, Nanotechnology 23 (2012) 385702.
[106] D. Yang, F. Ma, Y. Sun, T. Hu, K. Xu, Influence of typical defects on thermal conductivity of graphene nanoribbons: an equilibrium molecular dynamics simulation, Appl. Surf. Sci. 258 (2012) 9926–9931.
[107] C. Yu, G. Zhang, Impacts of length and geometry deformation on thermal conductivity of graphene nanoribbons, J. Appl. Phys. 113 (2013) 044306.
[108] Ning Wei, Lanqing Xu, Hui-Qiong Wang, Jin-Cheng Zheng, Strain engineering of thermal conductivity in graphene sheets and nanoribbons: a demonstration of magic flexibility, Nanotechnology 22 (2011) 105705.
[109] Haiying Yang, Yunqing Tang, Yu Liu, Xingang Yu, Ping Yang, Thermal conductivity of graphene nanoribbons with defects and nitrogen doping, React. Funct. Polym. 79 (2014) 29–35.
[110] Hang Zhang, Chengyun Hua, Ding Ding, Austin J. Minnich, Length dependent thermal conductivity measurements yield phonon mean free path spectra in nanostructures, Sci. Rep. (2015), http://dx.doi.org/10.1038/srep09121.
[111] Yogesh Sonvane, Sanjeev K. Gupta, Pooja Raval, Igor Lukacevic, Pankajsinh B. Thakor, Length, width and roughness dependent thermal conductivity of graphene nanoribbons, Chem. Phys. Lett. 634 (2015) 16–19.
[112] Z. Aksamija, I. Knezevic, Thermal transport in graphene nanoribbons supported on SiO_2, Phys. Rev. B 86 (2012) 165426.
[113] H.-Y. Cao, Z.-X. Guo, H. Xiang, Z.-G. Gong, Layer and size dependence of thermal conductivity in multilayer graphene, Phys. Lett. A 373 (2012) 525–528.
[114] Haoxue Han, Yong Zhang, Zainelabideen Y. Mijbil, Hatef Sadeghi, Yuxiang Ni, Shiyun Xiong, Kimmo Saaskilahti, Steven Bailey, Yuriy A. Kosevich, Johan Liu, Colin J. Lambert, Sebastian Volz, Functionalization mediates heat transport in graphene nanoakes, arXiv:1508.01616v1, 7 Aug 2015.
[115] D.D.L. Chung, Materials for thermal conductivity, Appl. Therm. Eng. 21 (2001) 1593–1605.
[116] P.G. Klemens, Theory of thermal conduction in thin ceramic films, Int. J. Thermophys. 22 (2001) 265–275.
[117] M.M. Sadeghi, M.T. Pettes, Thermal transport in graphene, Solid State Commun. 152 (2012) 1321–1330.
[118] D.-H. Chae, B. Krauss, K. von Klitzing, J.H. Smet, Hot phonons in an electrically biased graphene constriction, Nano Lett. 10 (2010) 466–471.
[119] A. Das, S. Pisana, B. Chakraborty, S. Piscanec, S.K. Saha, U.V. Waghmare, K.S. Novoselov, H.R. Krishnamurthy, A.K. Geim, A.C. Ferrari, A.K. Sood, Monitoring dopants by Raman scattering in an electrochemically top-gated graphene transistor, Nat. Nanotechnol. 3 (2008) 210–215.
[120] G. Chen, C.L. Tien, X. Wu, J.S. Smith, Measurement of thermal diffusivity of GaAs/AlGaAs thin-film structures, J. Heat Transfer 116 (1994) 325–331.
[121] C.L. Tien, G. Chen, Challenges in microscale conductive and radiative heat transfer, J. Heat Transfer 116 (1994) 799–807.
[122] X.Y. Yu, G. Chen, A. Verma, J.S. Smith, Temperature dependence of thermophysical properties of GaAs/AlAs periodic structure, Appl. Phys. Lett. 67 (1995) 3554–3556.
[123] J. Piprek, Thermal conductivity reduction in GaAs–AlAs distributed Bragg reflectors, IEEE Photonics Technol. Lett. 10 (1998) 81–83.